Environmental Science Processes & Impacts

ROYAL SOCIETY OF CHEMISTRY

PAPER

View Article Online
View Journal | View Issue

Cite this: *Environ. Sci.: Processes Impacts*, 2025, **27**, 3246

Mercury transfer and transformation from mine soil to river sediments: the potential role of amorphous iron oxides in methylation processes in southern Burkina Faso

D. Dabré, *[ab] S. Guédron,[a] Y. Maïga,[b] S. Jelavic,[a] S. Campillo,[a] J. Fin,[a] S. Sentenac,[a] O. Bruneel,[cd] O. Ouédraogo[b] and R. Mason[e]

Since the early 2000s, artisanal and small-scale gold mining (ASGM) has rapidly expanded in Burkina Faso. Mercury (Hg) is widely used to extract gold and its release through burning amalgams has led to soil contamination near mining sites. However, the fate and speciation of Hg in soils remains poorly understood, especially the reactivity or methylation potential of soil particles eroded into rivers. In this study, Hg contamination levels and speciation were assessed in water, soil, and sediments from five ASGM districts along the Mouhoun River. Surface waters near riverside mining sites showed high levels of particulate Hg (11–239 ng L^{-1}), while more arid sites showed Hg contamination localised to ore-washing ponds. Mercury thermodesorption and selective extraction analysis revealed that in soils collected in the vicinity of amalgam burning sites, around 10% of total Hg (THg) was elemental (Hg0), with most remaining Hg bound in the divalent state to amorphous iron oxides (~60% THg) and organic matter (~30% THg). In river sediments, Hg bound to amorphous iron was halved, while methyl Hg (MeHg) levels increased fivefold (0.7 ± 0.2 ng g^{-1}) suggesting that iron reduction in sediments promotes MeHg production and accumulation. These results highlight the potential risks of Hg exposure for local communities and the need for regional Hg management in ASGM areas.

Received 2nd June 2025
Accepted 4th September 2025

DOI: 10.1039/d5em00426h

rsc.li/espi

Environmental significance

Artisanal and small-scale gold mining (ASGM) is one of the largest contributors to mercury (Hg) pollution in terrestrial and aquatic ecosystems worldwide. The Hg used for gold amalgamation is volatilized into the atmosphere or released into terrestrial ecosystems, where it can be transformed into methylmercury (MeHg) under reducing conditions in river sediments. This toxic molecule accumulates in food webs, ultimately exposing humans. In this work, we emphasize the significance of amorphous iron oxides in the retention of Hg in mine soils of Burkina Faso, and suggest they are prone to methylation once eroded into river sediments. By linking Hg chemical and solid speciation, we demonstrate the importance of this characterization in assessing the availability of Hg for methylation.

1. Introduction

Most artisanal and small-scale gold mining (ASGM) activities are located in the intertropical region, involving between 10 and 19 million miners across Asia, Africa and South America.[1] In comparison to Asia and South America, West Africa has experienced its most extensive gold rush during the last few decades. Gold (Au) is typically recovered by crushing Au-ores, washing it to isolate heavy gold particles, and then mixing it with elemental mercury (Hg0) to form an amalgam. Burning of amalgam to extract gold releases mercury (Hg) vapor into the surrounding environment, which exposes miners and their families to Hg related risks.[2,3] Globally, it is estimated that ASGM is responsible for around 40% of global atmospheric mercury (Hg) emissions.[4] Environmental Hg contamination around ASGM sites results from multiple pathways including the direct loss of liquid Hg to soils and rivers, the release of particulate-bound Hg into rivers, and the deposition of Hg vapor in the environment following amalgam burning.[5,6]

Previous studies in West Africa demonstrated high levels of Hg in ASGM topsoils with concentrations of up to 410 μg g^{-1} in Ghana[7] and 8 μg g^{-1} in Senegal.[6,8,9] High levels of Hg in river

[a]Univ. Grenoble Alpes, Univ. Savoie Mont Blanc, CNRS, IRD, IFSTTAR, ISTerre, 38000 Grenoble, France. E-mail: djamilatou.dabre@univ-grenoble-alpes.fr
[b]Université Joseph KI-ZERBO, Laboratoire de Microbiologie et Biotechnologie Microbienne (LAMBM), Laboratoire de Biologie et Écologie Animale (LBEA), 03 BP 7021 Ouagadougou 03, Burkina Faso
[c]HydroSciences Montpellier, University of Montpellier, CNRS, IRD, Montpellier, France
[d]Univ Nangui Abrogoua, Lab Biotechnol & Microbiol Aliments, 02 BP 801, Abidjan 02, Cote d'Ivoire
[e]Department of Marine Sciences, University of Connecticut, 1080 Shennecossett Road, Groton, Connecticut 06340, USA

sediments close to ASGM sites have also been reported, reaching up to 10 μg g^{-1} in Senegal,[9] 5.4 μg g^{-1} in Tanzania, 2.9 μg g^{-1} in Ghana, and 20.4 μg g^{-1} in Côte d'Ivoire,[10] compared to the geochemical background that is between 0.005 and 0.3 μg g^{-1}.[11–14] Such elevated Hg concentrations in sediments result from important release of particulate bound Hg from ASGM sites, together with liquid Hg droplets close to the ore washing sites.[6] Consistently, elevated Hg levels in unfiltered surface water have been reported surrounding mining areas in Ghana (28.7 to 420 ng L^{-1}), Côte d'Ivoire (6.6 to 53 ng L^{-1}), Senegal (5.8 to 974 ng L^{-1}), and Burkina Faso up to 21 ng L^{-1}.[6,12,15–17] Once in the aquatic system, inorganic mercury can be converted by microorganisms into methylmercury (MeHg), a toxic compound that bioaccumulates and biomagnifies in the trophic chain.[16,18–20]

However, very few studies have examined MeHg levels in West Africa near ASGM sites. Amongst available studies, data indicate high MeHg accumulation in river sediments, with a highest concentration of 8.0 ± 7.8 ng g^{-1} in Senegal,[6] and between 0.7 and 4.3 ng g^{-1} in Cote d'Ivoire.[16] These studies indicated that MeHg levels are not related to total Hg concentration, but to sediment geochemical conditions. Consistently, highest MeHg concentrations are reported in suboxic to anoxic river sediments downstream of ASGM sites, as well as in ponds and shallow eutrophicated sites.[6,16] Hence, the release of Hg from ASGM sites into productive and stratified aquatic ecosystems, promotes the formation of MeHg.[21] It is therefore hypothesised that Hg-rich particles eroded from ASGM sites during mining operations or during the monsoon period supply downstream aquatic environments, where methylation occurs.

Despite the wide use of Hg in ASGM, little is known about the speciation and fate of Hg in iron-rich tropical soils, which dominate much of West Africa. Once deposited on the soil, Hg can be volatilised or complexed with organic matter and minerals, such as iron oxides and clay minerals.[22] Understanding the distribution of Hg between soil components is thus key to document the reactivity of Hg carrier phases, which are prone to (bio)reduction and (bio)methylation when deposited in river sediments.[23,24] During sediment diagenesis, organic matter degradation and Fe(III)-reduction are driven by microorganisms such as sulfate-reducing bacteria "SRB", iron-reducing bacteria "FeRB", and methanogens, some of which carry gene clusters putatively required for Hg methylation, *i.e. hgcA* and *hgcB*.[20,25] Other contaminants such as Pb and As can also be mobilised through ASGM operations either from ore dust emission[26] or pumped groundwater.[27]

In this study, the Hg speciation (*i.e.*, Hg0, THg and MeHg) and distribution in soils and river sediments was analysed across five ASGM sites along the Mouhoun River in southern Burkina Faso. We used thermodesorption experiments with selective extraction, grain size characterization and elemental chemical analysis to trace Hg from the mine to river environment. Comparative experiments between selective extraction and Hg thermodesorption experiments were also developed to test the reliability of thermal analysis applied to tropical soil and sediments. Finally, we document the levels of other geogenic contaminants such as As and Pb and examine the potential links between the contamination and site activity and history.

2. Materials and methods

2.1. Environmental settings

Burkina Faso (BF) is located in West Africa, and bordered by Mali, Niger, Benin, Togo, Ghana and Côte d'Ivoire (Fig. 1A). Burkina Faso experiences a tropical climate divided into a dry season, from November to May with warmer temperatures (>40 °C) from March to May, and a rainy season from June to October.[28] The regional BF geology is dominated by Precambrian rocks, including granites, greenstone belts, and metamorphic formations of the West African Craton.[29,30] The greenstone belts are especially rich in gold deposits. Most of the informal or small-scale gold mining activities in the country extract ores from these belts by digging. These sites vary in age, size and the numbers of miners involved. After extraction, the ore is milled both manually and using small stone crushers. Milled ores are then washed using either groundwater or surface water, depending on availability, to separate light particles from denser gold-bearing fractions using sluices. Gold particles are then concentrated through amalgamation with liquid Hg. The resulting amalgam is then burnt on site or in nearby houses to extract the gold. While most of these sites rely solely on the Hg-based amalgamation technique, some sites also employ cyanidation using sodium cyanide. Details of the extraction processes are provided in the SI (Fig. S1).

2.2. Sample collection and conditioning

Sampling was carried out in the south-western part of Burkina Faso during two field campaigns performed in May/June 2018 (sites detailed in Table S1), and the second in November 2022 as a part of the survey led by Agence Nationale d'Encadrement des Exploitations Minières Artisanales et Semi – mécanisés (ANEEMAS). The November 2022 campaign focused on five ASGM sites along the Mouhoun River (Fig. 1C) just before the access to these sites was restricted because of terrorist groups' activity. The studied area encompasses three main districts: (i) the rural district of Boromo, covering the mines of Siby (site B1) and Siggnonghin (B2); (ii) the urban district of Dano covering the mining areas of Gnikpière (B3) and Memer (B4); and (iii) the urban district of Gaoua including the mines of Djikando (B5), the Quadaradouo (B6), and the neighboring small mines of Bandediera, Banfara and Poniro (B7).

To document the environmental impact of these mining activities, surface water (Poni River and a pristine intermittent river at Dano, 3 km from the mining sites) and groundwater (wells and boreholes) were sampled at each site and in downstream villages in the 2022 campaign. At the same time, physicochemical parameters (pH, E_h, conductivity, turbidity) were measured using a multiparameter probe, Hach® (HQ4300).

Sampling was performed following an ultra-trace sampling procedure. At each sampling site, samples were collected in 250 mL FEP Teflon containers, and filtered with 0.45 μm sterivex filters (Millipore). Unfiltered (UNF) and filtered (F) samples for THg and MeHg analyses were transferred to 125 mL FEP vials, and acidified with HCl (0.5% v/v, trace grade – Baker). Filtered water samples for major (Fe, Al, S, Mn and P) and trace

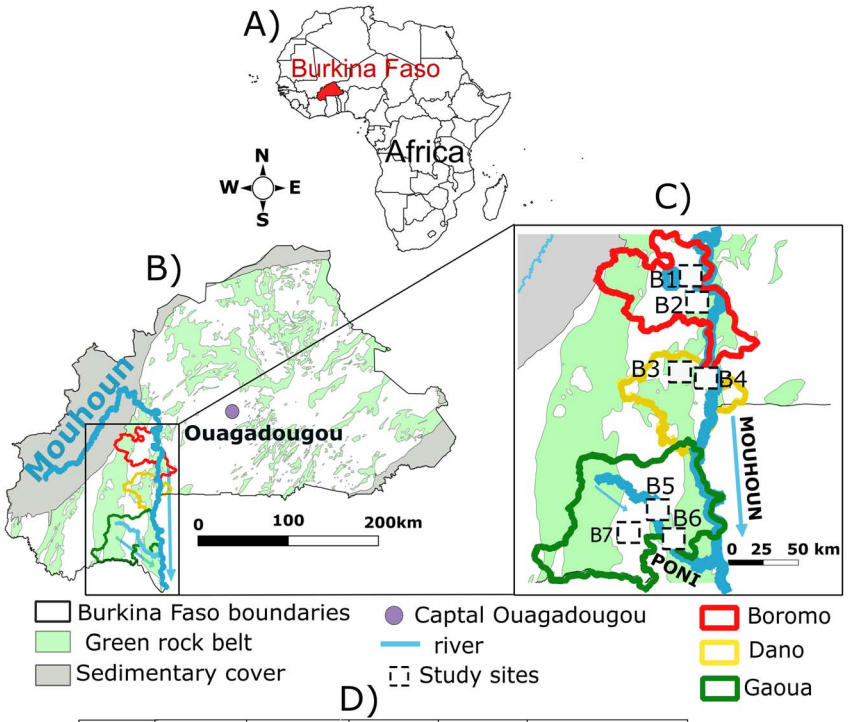

D)

Mining Sites	ASGM type	Miners (individuals)	Creation year	Surface (ha)	Water use in mining process
B1	Hg	~300	2009	6	River
B2	Hg+CN	~1000	2006	24	Groundwater
B3	Hg	~300	2019	100	Groundwater
B4	Hg	~500	1997	100	Groundwater
B5	Hg	~1200	1995	100	River
B6	Hg	N.D	N.D	N.D	Groundwater
B7	Hg	N.D	N.D	N.D	Groundwater

Fig. 1 Map of the study site with (A) the location of Burkina Faso within Africa. (B) Geological map of Burkina Faso showing the greenstone belt, the Mouhoun and Poni rivers, and the three studied mining districts: Boromo, Dano and Gaoua. (C) Zoomed in excerpt. (D) Synthetic information for all studied sites about the type of ASGM extraction process (mercury and or cyanidation), the number of miners, year of set-up, surface area at the date of sampling, and source of water used in the mining process.

element (As, Pb) analysis were stored in trace-grade 15 mL polyethylene falcon tubes, acidified with HNO_3 (2% v/v, trace-grade – Baker). Additional filtered water samples for anions (sulphate, chloride and phosphate) were stored frozen until analysis. For dissolved organic carbon (DOC) analysis, filtered water samples were collected in pre-burnt (550 °C for 3 hours) 20 mL amber borosilicate vials, and acidified with HCl (0.1 N) following published protocols.[31] All samples were packed in double bags and stored at 6 °C in the dark until analysis.

To assess the Hg levels throughout the Au extraction process, samples of primary rocks, milled ores, waste piles, and solid concentrates remaining after ore washing were collected in 2018 at the B6 and B7 mining sites. During the 2022 campaign, soils and sediments were collected at the B1 to B5 mining sites. At each site, a composite surface soil sample (0–5 cm depth) was collected by pooling 5 sub-samples over ~12 m^2 and stored in Whirl pack® sterile bags. These samples were homogenized in the bag and kept at room temperature until returned to the laboratory. Surface river sediments (0–5 cm depth) were collected with a polyethylene shovel from riverbanks, stored in Whirl pack® sterile bags, homogenized, and kept cool at 4 °C until analysis.

2.3. Soil and sediment characterization

In the laboratory, soil and sediment samples were freeze-dried, and dry sieved to recover the sand (0.5–2 mm), and clay + silt (<0.5 mm) granulometric fractions. Each fraction was weighed to determine its relative proportion. An aliquot was then ground into a fine powder (<63 μm) for chemical analysis.

X-ray diffraction (XRD) was carried out on the clay + silt fraction, to determine mineral phases using the PROFEX free-ware following a published protocol.[32]

2.4. Chemical analyses

2.4.1 Elemental analysis. Total Hg concentrations in filtered (THg_F) and unfiltered (THg_{UNF}) water were determined by cold vapor atomic fluorescence spectrometry (CV-AFS) after conversion of all Hg species into Hg0 followed by detection using a Tekran® Model 2500.[23,24] Quality assurance, quality control (QA/QC) was ensured using a certified reference material (ORMS-5), with THg concentrations obtained for repeated analyses (27.1 ± 0.6 ng L^{-1}, $N = 3$) always within the range of certified value (26.2 ± 1.3 ng L^{-1}). Field and analytical blank values for THg were 0.7 ± 0.3 ng L^{-1}, attesting to the absence of contamination during sampling and filtration in the field. The detection limit (DL) defined as 3 times the standard deviation of 10 blanks was 0.04 ng L^{-1}.

Total mercury analysis (THg) in solids (soil and sediment) was performed by atomic absorption spectroscopy (AAS) after pyrolysis at 550 °C and gold amalgamation (AMA 254, Altec) with a relative precision of ±5% determined from triplicates. The concentrations of THg obtained for repeated analyses of certified international reference materials ERM CC 141 [European Commission; 0.078 ± 0.003 μg g^{-1}, ($N = 7$)] and IAEA 158 [International Atomic Energy Agency; 0.123 ± 0.002 μg g^{-1}, ($N = 3$)] never exceeded the certified range published (*i.e.*, ERM CC 141 = 0.083 ± 0.017 μg g^{-1}, and IAEA 158 = 0.132 ± 0.014 μg g^{-1}, respectively). THg in mine waste solid samples was analysed by AAS after pyrolysis at 550 °C and gold amalgamation using a Nippon DMA-3000, following a published procedure.[33] Briefly, ~1 g of sample was digested in 5 mL of *aqua regia* overnight before analysis. QA/QC was ensured using the standard reference material MESS-4 (marine sediment SRM from NRC; 0.079 ± 0.001 μg g^{-1}), with relative standard deviation (% RSD) below 5%. For waste piles, rock and concentrate, including samples where Hg was added by miners, %RSD was <15%, given the inherent inhomogeneity of these samples.

Methylmercury concentrations in the filtered ($MeHg_F$) and unfiltered ($MeHg_{UNF}$) water samples were analyzed using an ethylation purge and trap gas-chromatograph (GC-CVAFS) analysis (Tekran®, model 2700) following published protocols.[34–36] The results were validated by duplicate analysis and quantification using the standard addition technique.[37] Field and analytical blank values were 0.038 ± 0.004 ng MeHg per L, attesting to the absence of contamination during field sampling, filtration and laboratory analysis. The detection limit (DL) was 0.01 ng MeHg per L. MeHg concentrations in soil were determined by the same method after acid digestion following published protocols.[38,39] Briefly, a mass of ~2 g was digested with 5 mL KBr (18%), 1 mL of 1 M $CuSO_4$ and 10 mL DCM (dichloromethane). 0.5 mL of DCM containing MeHg was then diluted in 30 mL milliQ water, and purged with argon for 30 minutes to remove all traces of DCM.[40,41] QA/QC was checked with triplicate analysis of reference material ERM CC 580 (74.8 ± 2.4 ng MeHg per g), which was within the range of certified values (74 ± 4 ng MeHg per g).

The concentrations of major (Al, Ca, Fe, Mg, Mn, S, Ti) and trace (Pb, Cu, Zn, Cd, Cr, As, Se) elements were analysed in filtered water and solids using an ICP-AES (Agilent, Varian 720-ES) and ICP-MS (Agilent, 7900), respectively, after total microwave digestion for solids (ultraWAVE, Milestone) at 250 °C as described by Falciani *et al.* (2000) and Melaku *et al.* (2005).[42,43] For filtered water, QA/QC was assessed through the analysis of the certified standards SLRS4 and SLRS6. For solids, QA/QC was assessed by the analysis of certified reference materials JSD3, IAEA-405 and BR24 for the sediment samples, and ERM CC 141 for the soils. Accuracies were always within the range of certified values with a ±5% margin of error.

The concentrations of major anions (Cl^-, NO_2^-, NO_3^-, PO_4^{3-}, SO_4^{2-}) were determined by ion chromatography (Dionex ICS 2000) controlled by the Chromeleon® chromatographic management system following a published protocol.[44]

Dissolved organic matter (DOC) was measured using a TOC-VCSN analyzer (Shimadzu®) as described by Tisserand *et al.* (2022, 2024).[45,46] Precision and recovery rate were better than 5%. Total carbon (TC), total organic carbon (C_{org}) content and isotopic signatures ($\delta^{13}C_{bulk}$ and $\delta^{13}C_{org}$) was determined on the silty-clay fraction, using Cavity Ring-Down Spectrometry (Picarro, Inc.®) coupled with a Combustion Module (Costech, Inc.®) (CM-CRDS) using the analytical method described in Guédron *et al.* (2019).[47] QA/QC was performed using a reference material, PACS-2 (certified value: $\delta^{13}C = -23.07 \pm 0.6$).

2.4.2 Mercury thermodesorption experiments. Mercury thermodesorption experiments on soil and sediment samples were performed following published protocols.[48,49] Briefly, 50 to 100 mg of soil and sediments (depending on the initial Hg concentration) were heated successively in an oven for 48 hours at 80 °C for the determination of Hg0,[50] then at 180 °C for the determination of Hg bound to organic matter (Hg_{180}), and finally by heating at 550 °C for the determination of Hg bound to refractory phases (Hg_{Res}). The concentration of Hg associated with each of these fraction was then obtained from the difference between THg in the bulk sample and the residue of pyrolysis as previously published.[22]

2.4.3 Selective extraction experiment. Two selective extractions were carried out on soil and sediment samples to identify and quantify the main Hg-bearing phases. The Hg bound to the organic matter (OM) was extracted by adding 4 mL of NH_4OH (1 M) to 40 mg of samples[51,52] under stirring. Extraction of the Hg bound to poorly crystallised Fe(III) oxide minerals and ferrihydrite was carried out by adding ascorbate to approximately 40 mg of the sample aliquot stirred at room temperature for 24 hours.[53,54] The entire analysis protocol is presented in previous publications.[22,51,55] Briefly, experiments were carried out in 15 mL trace grade vials at a solid/liquid ratio of 1 : 100.[52] At the end of the extraction time, samples were centrifuged (3000 rpm for 20 min), the supernatant was analyzed for major elements, and the solid residue was freeze-dried before Hg analysis. Complementary experiments were also performed to verify that the two selective extractions effectively remove Hg0. The NH_4OH or ascorbate selective extractions were thus performed both before (before T80) and after thermo-desorption at 80 °C (after T80).

2.5. Statistical analysis

Because geochemical data were not normally distributed, the geochemical dataset reported in this manuscript is presented as

the mean, the median and the standard error of the mean (SEM), [mean (median) ± SEM], and the number of observations (N).[56] In addition, non-parametric Mann–Whitney rank sum test (U test) and Kruskal–Wallis one-way analysis of variance on ranks (H test) were used to compare two or more than two data sets, respectively. Pearson correlations were applied to compare multiple data set pairs. The correlation coefficient (R^2) and p values (p) are reported. All statistical treatments were performed with R software (R.4.4.1), Sigmaplot and Sigmastat® software.

3. Results and interpretations

3.1. Mercury, arsenic and lead contents in surface and groundwater

Across all studied sites, both surface water (river) and groundwater exhibited close to neutral pH, averaging 7.3 (7.4) ± 0.1 (Table 1). Concentrations of phosphate, nitrate and DOC remained relatively low in river water, indicating limited influence of anthropogenic activities such as domestic wastewater discharge or agricultural runoff. In contrast, water used for ore processing was slightly more alkaline with an average pH of 8.3 (8.3) ± 0.2 (Table 1).

Groundwaters also exhibited the highest electrical conductivity values, which increased from north to south. The highest conductivity was measured at Gaoua (site B5, up to 900 μS cm^{-1} in groundwater, and 507 μS cm^{-1} in river), the oldest site in the study (active since 1995), which covers a large area (100 ha) and supports a dense mining population of around 1200 workers. Upstream at Boromo and Dano, although conductivity is lower, high sulfate levels are found in groundwater suggesting the release of sulfate from sulphide mineral oxidation (*i.e.*, pyrite) in groundwater.[57,58]

Total mercury concentrations in filtered water (THg_F) are low, with the lowest values in groundwater (0.1 to 2 ng L^{-1}) and the highest in mining effluents (0.9 to 6.5 ng L^{-1}) and surface water (2 to 8 ng L^{-1}). Highest THg concentrations are found in surface water at Boromo (8 ng L^{-1}) and in mine water from Dano's washing tanks (6.5 ng L^{-1}). Meanwhile, methylmercury represents 11 to 20% of THg in mine water (washing tanks and mine drainage), and 11 to 35% in filtered groundwater. In filtered river water, methylmercury remains below 3% of THg, except in Gaoua, where it exceeds 10%, highlighting a localized increase in methylation processes. Total mercury concentration in unfiltered surface water (THg_{UNF} = between 11.6 and 239 ng L^{-1}) are 4 to 27 times higher than filtered concentrations (between 2.7 and 8.7 ng L^{-1}), and rise with turbidity levels, notably at Boromo (B1, THg_{UNF} = 239 ng L^{-1}, Turb = 459 NTU) and Gaoua (B5, THg_{UNF} = 37 ng L^{-1}, Turb = 152 NTU), where river water is used for ore processing. This highlights that Hg is mainly associated with suspended particles (Fig. S2). In unfiltered river and mine water, methylmercury (MeHg) represents less than 6% of THg, whereas in groundwater, it accounts for 10 to 30%, indicating different partitioning of MeHg between water and particles.

Finally, in ASGM locations where surface water is not available (Fig. 1), the pumping of water from geogenically enriched lead (Pb) and arsenic (As) substrates can lead to co-contamination of surface waters. Concentrations in As and Pb in filtered water are low at most sites (Table S2) and with both water types, with average concentrations of 1.6 (0.7) ± 0.7 μg L^{-1}. Only the site of Dano (B4) exhibits high As levels in groundwater reaching 61 μg L^{-1}, which is consistently found in the water used for ore washing (140 μg L^{-1}, Table 1).

3.2. Mercury, arsenic and lead levels in soils and sediments

Total mercury levels in rocks and lateritic soils are low, *i.e.*, from 0.001 to 0.02 μg g^{-1} (Table 2), and in the range of the geochemical background in pristine environments in Ghana.[59] In organic matter poor topsoil (*i.e.*, C_{org} from 0.3 to 1.4 μg g^{-1}, Table 2) with highly humidified OM (C/N = 17 ± 2, Table S5) located over 2 km from ASGM sites, THg concentration were slightly higher, averaging 0.3 (0.3) ± 0.1 μg g^{-1} (Table 2). These value are close to those reported for pristine soils in western Africa [*i.e.*, < 0.3 μg g^{-1} (ref. 60)], and fall within the range reported in South American pristine soils [0.01 to 0.49 and 0.9 μg g^{-1} (ref. 22 and 61)], but higher than the values reported for cropland soil in Burkina Faso [0.03 ± 0.01 μg g^{-1} (ref. 62)].

Similarly, THg concentrations in sediments upstream of mining sites are low, between 0.05 and 0.3 μg g^{-1}, consistent with natural background levels. In contrast, THg levels in mining areas are 4.5 to 22 times higher, with the highest concentration found in mine waste and ore concentrates, which exhibit THg values between 7.4 (3.1) ± 5.5 and 2.2 (2.2) ± 1.6 μg g^{-1}, respectively (Table S1). The most extreme THg concentration is observed in Hg-amalgamated ore concentrates at Gaoua, where THg levels average 4147 (2056) ± 2725 μg g^{-1}. Similarly, THg concentrations in ASGM topsoils vary between 0.9 and 4.5 μg g^{-1}, which is substantially higher compared to reference soils. In contrast, THg levels in river sediment are moderate (0.1 (0.1) ± 0.04 μg g^{-1}, Table 2), except for the ore washing site at Gaoua, where THg concentrations reach up to 7.8 μg g^{-1}. The majority of THg in soils is associated with the silty-clay granulometric fraction (75 (83) ± 4% of THg). In sediments, however, the THg is equally represented in the clay + silt fraction (53 (47) ± 7%) compared to sand fraction (47 (53) ± 7%).

Methylmercury (MeHg) concentrations in soils are overall low and range from 0.04 to 0.3 ng g^{-1}, with no significant difference between reference soils and ASGM-impacted soils. MeHg constitutes <0.1% of THg, indicating limited methylation in these environments. In sediments, MeHg percentages are at least five times higher compared to soils with higher MeHg concentrations (0.7 (0.8) ± 0.2 ng g^{-1}) suggesting enhanced MeHg accumulation in sediments. In addition, the sediment collected at the site with low THg concentration (*i.e.*, Dano, B3-3) had a lower proportion of MeHg than those collected downstream of ASGM sites.

Lead (Pb) concentrations in soils were low (17.9 (10.1) ± 4.7 μg g^{-1}), falling within the geochemical background range of 4–35 μg g^{-1} as previously reported.[63–66] Arsenic (As) levels were similarly low (3.3 (2.4) ± 1.3 μg g^{-1}, Table 2), with the exception of the Dano ASGM site, where concentrations reached up to 87 μg g^{-1}. Consistently, both As and Pb concentrations in

Table 1 Physico-chemical parameters and metal(loid) concentrations in filtered and unfiltered water in Boromo, Dano and Gaoua districts[a]

Filtered water

Sample	District	Site	pH	SO_4^{2-} (mg L^{-1})	DOC (mg L^{-1})	THgF (ng L^{-1})	MeHgF (ng L^{-1})	As (μg L^{-1})	Pb (μg L^{-1})
River	Boromo	B1°	7.2	0.9	4.2	8.7	0.2	1.2	1.0
	Dano*	B3	7.5	0.9	1.4	2.7	0.03	0.4	0.06
	Gaoua	B5° ($N = 3$)	7.2 (7.11) ± 0.1	3.7 (2.1) ± 1.7	2.2 (2.0) ± 0.7	4.6 (2.7) ± 2.0	0.6 (0.5) ± 0.2	0.5 (0.4) ± 0.1	0.06 (0.05) ± 0.01
Groundwater	Boromo	B2	6.5	3.0	0.3	2.3	0.8	0.2	0.1
	Dano	B3 ($N = 2$)	7.8	1.3 (1.3) ± 0.03	0.3 (0.3) ± 0.03	1.4 (1.4) ± 0.3	0.5 (0.5) ± 0.3	5.1 (5.1) ± 0.6	0.02
	Dano	B4	7.9	14.1	0.2	0.1	N.D	61	0.06
	Gaoua	B5°	7.4	<DL	0.5	1.2	0.3	1.4	0.03
Water used in the mining process	Boromo	B2	8.0	0.8	1.5	0.9	0.1	1.6	0.1
	Dano	B4	8.5	3.0	1.5	6.5	1.3	140	0.1

Unfiltered water

			Turb (NTU)	Cond (μS cm^{-1})	THg_{UNF} (ng L^{-1})	$MeHg_{UNF}$ (ng L^{-1})
River	Boromo	B1°	454	80	239	0.1
	Dano	B3	57	70	11.6	0.6
	Gaoua	B5° ($N = 3$)	152 (132) ± 36	540 (560) ± 248	37 (23) ± 18	1.2 (1.0) ± 0.6
Groundwater	Boromo	B2	14.1	120	N.D	N.D
	Dano	B3 ($N = 2$)	11.1	250	2.4 (2.4) ± 0.4	0.7
	Dano	B4	10.8	320	3.0	0.4
	Gaoua	B5°	11.0	940	3.7	0.7
Water used in the mining process	Boromo	B2	84	210	16.6	0.4
	Dano	B4	136	260	50.7	0.2

[a] * indicates pristine river water collected 3 km away from the mining Dano site. ° indicates sites where river water is used for ore processing whereas the others use groundwater. The SEM only appears when there are at least two values. N.D indicates not determined.

Table 2 : Concentrations of metal(loids) in crushed rock, soils, sediments, concentrate, concentrate to which mercury has been added, and waste material for sites in the districts of Boromo, Dano and Gaoua. Concentrations are given in dry weight. N.D indicates not determined, and <DL indicates below detection limits. The SEM only appears when there are at least two values[a]

Soils, rocks and sediments								
Type	District	C_{org} (%)	THg in clay & silt (%)	THg in sand (%)	THg ($\mu g\ g^{-1}$)	MeHg ($ng\ g^{-1}$)	As ($\mu g\ g^{-1}$)	Pb ($\mu g\ g^{-1}$)
Green belt rocks	Boromo ($N = 4$)	N.D	N.D	N.D	0.006 (0.002) ± 0.005	N.D	<DL	<DL
Soil outside mine	All* ($N = 3$)	0.8 (0.7) ± 0.1	66 (68) ± 9	34 (32) ± 9	0.3 (0.3) ± 0.1	0.1 (0.1) ± 0.08	47.2 (2.8) ± 45.1	11.7 (8.4) ± 5.4
Mining soils	Boromo ($N = 3$)	0.3 (0.3) ± 0.04	85 (83) ± 3	15 (17) ± 3	2.3 (0.2) ± 2.1	0.04 (0.04) ± 0.01	3.4 (1.8) ± 1.8	14.8 (8.1) ± 6.9
	Dano ($N = 4$)	1.4 (1.5) ± 0.2	72 (75) ± 6	28 (25) ± 6	4.5 (1.5) ± 3.5	0.2 (0.1) ± 0.1	87 (77) ± 44	28 (23) ± 10
	Gaoua	0.9	84	16	0.9	0.3	3	5.7
Waste pile	Gaoua ($N = 3$)	N.D	N.D	N.D	7.4 (3.1) ± 5.5	N.D	N.D	N.D
Concentrate	Gaoua ($N = 2$)	N.D	N.D	N.D	2.2 (2.2) ± 1.6	N.D	N.D	N.D
Concentrate + Hg	Gaoua ($N = 4$)	N.D	N.D	N.D	4147 (2056) ± 2725	N.D	N.D	N.D
Sediment	Boromo	0.4	54	46	0.17	0.9	1.9	9
(upstream ASGM)	Dano ($N = 2$)	1.7 (1.7) ± 0.1	64 (64) ± 20	36 (36) ± 20	0.05 (0.05) ± 0.01	0.08	4.6 (4.6) ± 0.3	8.5 (8.5) ± 0.1
	Gaoua	1.2	50	50	0.3	0.8	6.7	13.8
Sediment	Gaoua	1.4	45	55	7.8	1.5	10.6	18.8
(ASGM ore leaching area)								
Sediment	Gaoua	1.2	40	60	0.1	0.2	5	10
(downstream ASGM)								

[a] * indicates all three studied districts (Boromo, Dano and Gaoua).

sediments were generally low, except at the Gaoua ore leaching site, where they reached 10.6 and 18.8 $\mu g\ g^{-1}$. These localized hotspots likely reflect contamination linked to naturally enriched ores and site-specific ore processing activities.

3.3. Mercury speciation and carrier phases in soils and sediments

Elemental mercury (Hg0) quantified by thermodesorption at 80 °C (Fig. 2) averaged 10 (9) ± 3% THg in pristine soils, and increased moderately at ASGM sites (15 (7) ± 6% THg), with higher levels at Boromo (B1-1 and B2-1) and Dano (B4-1), where Hg0 reached up to 57% THg. In river sediments, although THg concentrations were lower than in soils, except at Gaoua ore washing area (B5-3), Hg0 still averaged 8 (8) ± 1% THg in pristine sediments, and 12 (11) ± 2% THg downstream of ASGM sites.

To verify that the two selective extractions (NH_4OH or ascorbate) effectively remove Hg0, they were performed both before (before T80) and after thermo-desorption at 80 °C (after T80). In all cases, the THg recovered before T80 equalled the sum of the THg recovered by thermodesorption at 80 °C plus THg recovered after T80, confirming that both extractants also extracted Hg0 present in soils and sediments (Fig. S3). Hence, in the remainder of the manuscript, reference to NH_4OH extraction performed after thermodesorption will be referred to as Hg_{OM}, and ascorbate extraction performed after T80 will be referred to as Hg_{amFe}.

Hg_{OM} in pristine soil corresponded to 40 (38) ± 5% of THg, while in ASGM soil it corresponded to 32 (29) ± 4% (Fig. 2). In contrast, Hg_{amFe} is more abundant in both cases (59 (58) ± 2%) in pristine soils and ASGM soils (57 (57) ± 3%), suggesting that amorphous or weakly crystalline iron oxides such as ferrihydrite likely dominate Hg partitioning in soil.[53]

In river sediment, Hg_{OM} was higher in pristine samples (46 (46) ± 2% THg) than in sediment samples collected downstream from ASGM sites (26 (30) ± 9%). However, Hg_{amFe} remained similar between pristine (29 (29) ± 8% THg) and ASGM-influenced sediment (30 (31) ± 6% THg).

3.4. Comparison between thermodesorption and selective extractions

Thermodesorption has been used by many authors to identify Hg association with carrier phases in soils and sediments, providing an alternative to laborious sequential chemical extractions.[22,49,67–71] To test its reliability in these tropical soils and sediments, we compared Hg thermo-released at 180 °C (Hg_{180}), expected to represent divalent mercury bound to organic matter,[69,70] with results from NH_4OH and ascorbate extractions. Thermodesorption at 180 °C released 77 (89) ± 13% THg from pristine and 78 (86) ± 7% THg from ASGM soils (Fig. 3).

Hg_{180} showed a significant correlation with Hg_{OM} ($R^2 = 0.95$, $p < 0.01$) but the slope of the regression curve ($Hg_{OM} = 0.28Hg_{180} + 34.72$) suggests that only ~28% of Hg_{180} is Hg_{OM}, as quantified by the NH_4OH extraction (Fig. 3A). In contrast, Hg_{180} correlated more strongly with Hg_{amFe} ($R^2 = 0.99$, $p < 0.01$, Fig. 3B), with a larger regression slope ($Hg_{amFe} = 0.64Hg_{180} - 11.04$) indicating greater thermal recovery of Fe-bound Hg.

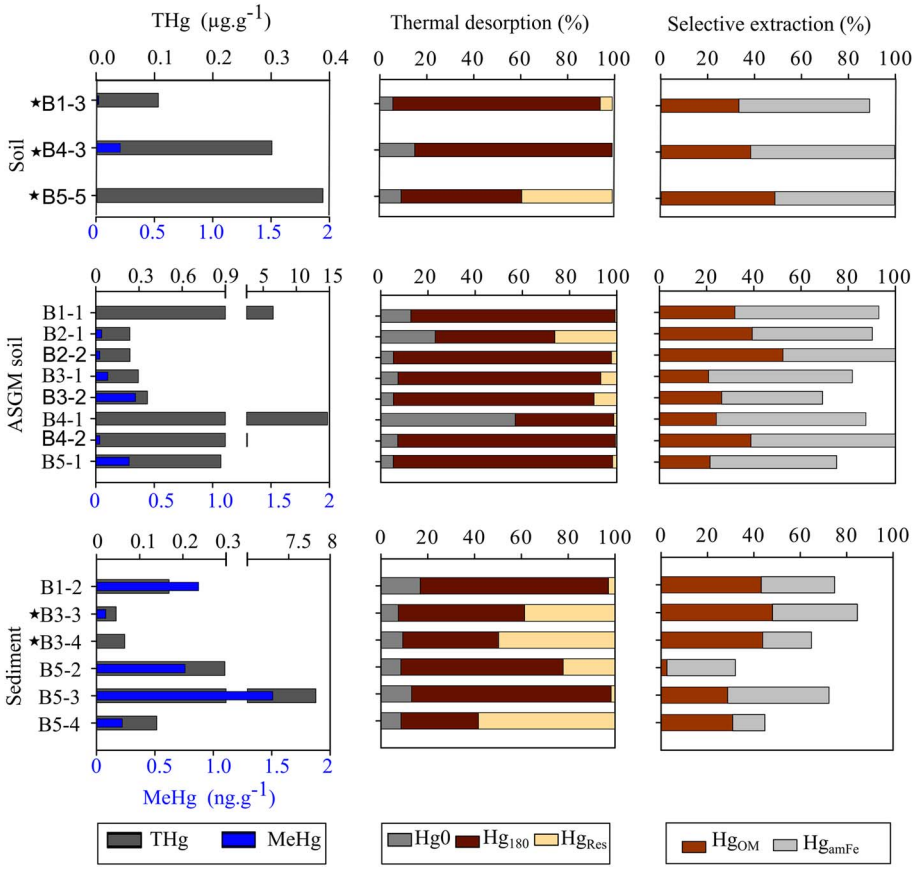

Fig. 2 From left to right: methylmercury (MeHg) and total mercury (THg) concentrations. Proportions of THg (%) released by thermodesorption at 80 °C (Hg0), 180 °C (Hg_{180}) and the difference between 180 and 550 °C (Hg_{Res}), NH_4OH (Hg_{OM}) or ascorbate (Hg_{amFe}) selective extraction in soil away from ASGM sites (top); ASGM-influenced soil (middle) and river sediment (bottom). Stars indicate the pristine environment, *i.e.*, soil samples at Boromo, Dano and Gaoua (Site B1-3, B4-3 and B5-5, respectively) were collected a few km downstream of the ASGM site, and sediment samples were collected upstream of the ASGM site at Dano (sites B3-3 and B3-4). All Gaoua sediment samples (site B5) were collected downstream of the ASGM site.

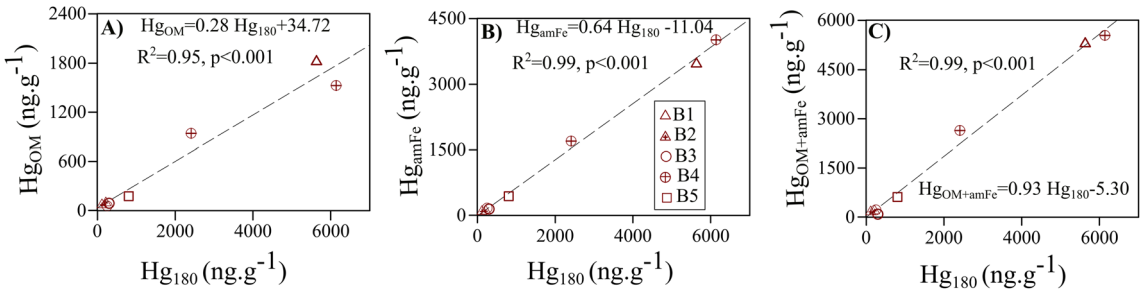

Fig. 3 ASGM soils. Biplots between Hg released by thermal desorption at 180 °C (Hg_{180}) and (A) Hg_{OM} (extracted by NH_4OH); (B) Hg_{amFe} (extracted by ascorbate) and (C) the sum of Hg_{OM} plus Hg_{amFe} ($Hg_{OM+amFe}$).

Finally, when Hg_{180} is compared to the sum of Hg_{OM} and Hg_{amFe}, the correlation remained high ($R^2 = 0.99$, $p < 0.001$, Fig. 3C) with a near unity slope ($(Hg_{OM} + Hg_{amFe}) = 0.93Hg_{180} - 5.30$), suggesting that treatment at 180 °C likely captures Hg associated with both OM and amorphous or weakly crystalline Fe oxides. In river sediments, Hg_{180} was lower than in pristine soils, averaging 47 (47) ± 6% in pristine samples and 67 (75) ± 12% in ASGM-influenced ones.

The residual divalent Hg (Hg_{Res}), defined as the difference between thermodesorption at 180 °C and 550 °C, was minor in soils, typically <6%. However, Hg_{Res} increased in river sediments, averaging 44 (44) ± 6% THg in pristine sediments and 23 (16) ± 13% downstream of ASGM sites.

Finally, from an analytic perspective, low-cost thermodesorption approves a valuable tool for analysis of West African tropical soils. Thermodesorption at 80 °C reliably captures Hg0,

while thermodesorption at 180 °C reflects Hg associated with both organic matter and amorphous iron oxides. However, distinguishing between those two fractions still requires selective chemical extractions.

4. Discussion

4.1. Impact of ASGM activities on mercury and arsenic contamination of surface water

Mercury concentrations in filtered groundwater and surface water (THg_F = 5.0 (2.7) ± 1.5 ng L^{-1}) across the three ASGM districts were comparable to background values reported for pristine surface water in BF (5.3 ± 6 ng L^{-1}),[17] and were lower than those reported downstream of ASGM areas in Senegal (5.6 to 34.5 ng L^{-1}).[6] The positive correlation found between THg_F and DOC ($R^2 = 0.74$, $p < 0.05$, Fig. S1 and Table S4) suggests that dissolved and colloidal Hg is mainly bound to organic ligands.[72,73] $MeHg_F$ concentration and contribution to THg_F (below 3%) aligned with observations in other surface waters of BF and Côte d'Ivoire.[16,17] In groundwater, THg_F and DOC do no show significant correlation ($p > 0.05$) suggesting that Hg is not only bound to organic ligands, but potentially to other inorganic ones (Table S3).

In contrast to filtered fractions, unfiltered surface and mine waters exhibited higher THg_{UNF} concentrations (up to 240 ng L^{-1}). These values were positively correlated with turbidity (0.97, $p < 0.01$), indicating that particulate-bound Hg is the main vector of Hg transport in aquatic systems.[6] The highest THg_{UNF} concentration was found at the Boromo site (B1), the most recent ASGM site (established in 2009), which has the lowest number of miners. In contrast, THg_{UNF} levels were lower at Gaoua (B5), the oldest ASGM and most intensively mined site (Fig. 1), likely because of the easier access to the Poni river, which dilutes the suspended solids and associated contamination. This suggests that local hydrographic conditions, particularly the river type (intermittent/permanent), play a larger role in controlling Hg mobilisation compared to size, age and the intensity of ASGM activities. For example, during the dry season, water levels in intermittent rivers like Boromo drop, resulting in minimal direct input of contaminated waters directly into surface waters.

In sites where the river is not accessible, miners rely on groundwater to wash ores. This practice supplies As-rich water to the surface, especially when geogenic As levels in groundwater are high. The green stone belt of BF contains sulfidic minerals such as pyrite and arsenopyrite, which are known sources of high concentrations of arsenic.[74] Elevated As levels in groundwater have been reported across the country, ranging from 0.2–140 µg L^{-1}.[27,75,76] A notable case is Dano, where As concentration in wells used for drinking water exceeded the WHO guidelines of 10 µg L^{-1},[77] posing a potential public health risk.[76,78] Groundwater samples from Dano revealed high As concentration (60 µg L^{-1}) along with high sulfate concentrations (14 mg L^{-1}), supporting that the oxidation of sulfidic minerals is the likely source of As in this region.

4.2. Partitioning of mercury species onto soil carrier phases in the ASGM context

Mercury concentrations in topsoils from ASGM sites (0.9 to 4.5 µg g^{-1}) were 3 to 15 times higher than those measured in non-ASGM sites (0.3 (0.3) ± 0.1 µg g^{-1}), which had similar levels to background levels reported for tropical soils in South Africa [0.075 to 0.15 µg g^{-1} (ref. 79)], West Africa [<DL to 0.19 µg g^{-1} (ref. 14)], New Zealand [0.018 to 0.339 µg g^{-1} (ref. 80)], Amazonia [0.01 to 0.9 µg g^{-1} (ref. 22 and 61)], and Australia [0.68 µg g^{-1} (ref. 81)]. Elemental mercury levels at (T80) in pristine topsoils (10 (9) ± 3% THg) are virtually the same as those in ASGM soil (9 (7) ± 2%, without sample B4-1). This shows that all the soils collected in this study contain at least ~10% Hg in the form of thermally unstable Hg reported to be represented mainly by Hg0, and small proportions of Hg chlorides.[49,82] The high amounts of Hg0 in ASGM topsoils (Fig. 2), in particular at Dano, suggest its deposition after condensation near amalgam burning sites.[6] Under BF's dry and warm climate, this accumulated Hg0 might be re-emitted into the atmosphere,[83] making these topsoils long term sources of atmospheric Hg0. Unfortunately, the limited number of collected topsoil samples in Hg0 contaminated sites, such as Dano, do not allow for the modelling of Hg0 re-emissions, which will need to be quantified in future research. In parallel, the presence of elemental mercury in river sediment downstream from mining sites (~10%, Fig. 2), also suggests transport of Hg0 from topsoils to the river during the wet season when erosion is most important.

In both pristine and ASGM soils, divalent Hg is mainly bound to amorphous or weakly crystalline Fe oxides (58 ± 3% THg), highlighting their major role in Hg retention.[22,84,85] Amorphous oxides are known for their high metal sorption capacity, particularly due to the significant contribution of intraparticle diffusion, and site densities as much as 3 orders of magnitude greater for amorphous iron oxide than for goethite.[86,87] This is further supported by the low proportion of Fe and Al extracted with ascorbate (<2% of total soil Fe or Al; Tables S5 and S6). Although ascorbate extraction has been reported to be highly selective and specific for amorphous oxides,[53,54,88] the potential dissolution to a small extent of metal–SOM complexes, and Fe oxides such as small amounts of goethite and hematite cannot be excluded.[88,89] In contrast to Amazonian soil, where divalent Hg is mainly associated with OM,[5,22] the BF soils exhibit a lower Hg-OM association (Hg_{OM} = 34 (33) ± 3% THg). Furthermore, a positive correlation between Hg_{OM} and total sulfur content in soils ($R^2 = 0.74$, $p < 0.05$, Fig. 4A) suggests that Hg is complexed with sulfur-containing functional groups in OM, which is consistent with the observations in Amazonian soils.[22] The agreement between Hg levels measured with thermo-desorption at 180 °C and the combined sum of Hg_{OM} and Hg_{amFe} likely indicates that the divalent Hg is associated with both OM and amorphous or weakly crystalline Fe oxides,[69] such as organic coatings on Fe/Al oxides, which have been described in the Amazonian region.[22,50,70]

Although the proportion of MeHg in soil was low (<0.1% HgT), a significant correlation with organic matter ($R^2 = 0.67$; $p < 0.05$, Fig. S4B) suggests that OM controls the MeHg

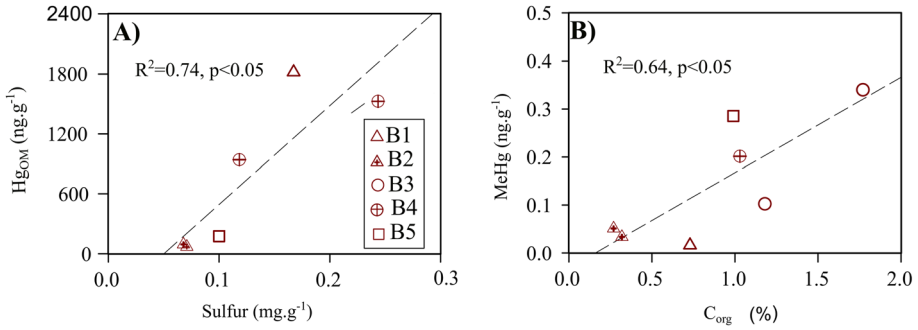

Fig. 4 ASGM soil. Biplots between (A) Hg_{OM} (extracted with NH_4OH) and total sulfur, (B) MeHg concentration *versus* organic carbon (C_{org}).

accumulation in soils, consistent with earlier studies.[90] Yet, the data on MeHg in tropical African soils remain scarce. The concentrations found in BF soils (0.13 (0.08) ± 0.04 ng g^{-1}) fall at the lower end of the range reported for Amazonian soil and litter [<1 ng g^{-1} (ref. 91)]. Such low MeHg levels likely reflect limited atmospheric MeHg input *via* throughfall and litterfall,[23,92] or unfavorable geochemical conditions for *in situ* methylation in arid conditions.[93]

Although crystalline Fe oxides (goethite and hematite), and kaolinite account for about a quarter (25 (24) ± 9%, Fig. S4) of the soil composition, the high proportion of Hg associated with amorphous iron oxides suggests that these crystalline iron oxides and clay minerals play a secondary role in Hg retention, in line with observations from Amazonian soils.[22] The remaining divalent Hg fraction (Hg_{Res} = THg − Hg_{180} − Hg0) correlated with Al concentrations (R^2 = 0.66, p < 0.05, Fig. S2). This suggests that HgRes is likely associated with aluminosilicates consistent with the silicate-rich soils composed mainly of quartz (40–80%) and kaolinite (5–30%), with minor amounts of minerals such as goethite, hematite, mica and others (Fig. S4).

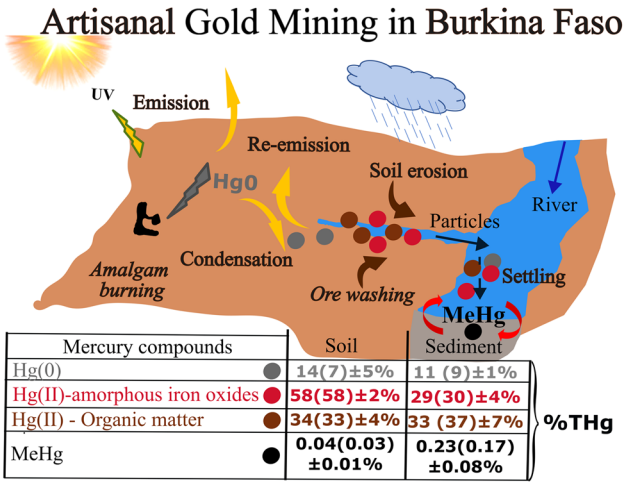

Fig. 5 Synthesis figure showing the environmental processes involved in gold mining and the percentages of different mercury compounds in soils and sediments downstream of mining sites in Burkina Faso.

4.3. Fate of Hg carrier phases and implication in MeHg accumulation in river sediment

Hg in ASGM soils is primarily associated with silt and clay size particles (Table S5), and these fractions are the most susceptible to erosion and downstream transport during the rainy season (Fig. 5). Once deposited in river sediments, amorphous and weakly-crystallized iron oxides – enriched in the clay fraction because of their small particle size, rapidly dissolve in reducing environments or get recycled by sediment microorganisms during early diagenesis.[6,94] This transformation enhances Hg availability for methylating organisms. Consistently, the proportion of Hg bound to amorphous or weakly crystalline oxides in sediments is at least twice as low compared to soil (all detailed in Table S7). This difference is offset by a five-fold increase in Hg associated with undefined mineral phases in the residual fraction (Hg_{Res} = 30 (30) ± 9% THg *vs.* Hg_{Res} = 9 (3) ± 4% THg in soil). Meanwhile, Hg associated with OM in sediments (Hg_{OM} = 33 (37) ± 7% THg) remains similar to soil values (Hg_{OM} = 34 (33) ± 3% THg). Thus, the decline in Hg_{amFe} without a rise in Hg_{OM}, offset by the rise in Hg_{Res}, suggests Hg released from the dissolution of amorphous iron oxides under anoxic conditions has been recycled onto diagenetically neoformed minerals.[24,95]

The percentage of MeHg in river sediments (0.23 (0.17) ± 0.08% THg) is at least five times higher compared to soils (0.04 (0.03) ± 0.01% THg) suggesting enhanced MeHg production and accumulation in river sediments.[6] It is therefore likely that some Hg released during sediment amorphous Fe oxide dissolution has becomes available for methylating microorganisms.[94,96] Although the presence of Hg associated with amorphous iron oxides is known to promote methylation,[94,97], (de)methylation rates in sediments are directly influenced by Hg biochemical availability, as well as by a large number of environmental variables, including biological and nutrient availability, pH, temperature, redox potential (*i.e.*, anaerobic conditions), and the presence of inorganic and organic (*e.g.*, inhibition due to sulphide formation) complexing agents.[98–101] All these environmental factors strongly influenced the metabolic activities of specific methylating microbes,[20] such as sulfate (SRB) and iron-reducing (IRB) bacteria.[25,96,102,103] Interestingly, MeHg percentages in sediments decreased as C_{org} increased (R^2 = 0.82, p < 0.05, Fig. S5) suggesting that Hg associated with OM is less bioavailable to methylating

organisms compared to Hg associated with reactive iron oxides.[24,94] In parallel, no significant correlation is found between THg and MeHg concentrations in sediments indicating that MeHg accumulation is independent of the amount of THg, but rather depends on the reactivity and type of Hg carrier phases,[23,24] the geochemical conditions (*e.g.*, redox),[6,16] and the types of microorganisms (*e.g.*, SRB and IRB) present in the system that carry gene clusters putatively required for Hg methylation.[20,25] In addition, even at highly contaminated sites, such as Gaoua sediments downstream of the ore washing area (THg = 7.8 μg g^{-1}), MeHg remains low. This likely results from the predominance of Hg in forms such as Hg0 (Hg0 = 13% THg) which are potentially less available for microbial methylation.

5. Conclusion

This study highlights that the recent expansion of artisanal and small-scale gold mining (ASGM) activities in Burkina Faso has a major impact on the Hg contamination in soils, especially near amalgam burning sites. The magnitude and the extent of contamination are closely related to local mining practices and the environmental context (access to river or groundwater for ore washing, and location of amalgam burning sites), rather than to the size or age of the ASGM sites and the number of miners.

River sediment contamination results from high particulate Hg release into rivers in areas where ore is processed directly on river banks. In contrast, groundwater-based ore processing limits downstream contamination, but increases the risk of arsenic mobilisation from bedrocks.

In ASGM soils, Hg0 accounts for approximately 15% of THg, and up to 57% in amalgamation areas. Divalent Hg is mostly bound to amorphous iron oxides (~60%) and organic matter (~30%). In contrast, in river sediments, amorphous iron oxide-bound Hg decreased sharply by five-fold, and methylmercury (MeHg) concentrations increased proportionally. Our findings suggest that once associated with amorphous iron oxides, Hg is likely more bioavailable to methylation in river sediments. By contrast, Hg associated with OM appears less bioavailable for methylating organisms.

Future research should focus on the fate of elemental Hg in soils, including volatilization rates, quantify exposure risks for nearby populations and miner communities, and investigate microbial communities responsible for MeHg production in river sediments. Experiments using isotopically enriched Hg adsorbed onto carrier phases such as amorphous Fe oxides could determine the conditions under which Hg becomes bioavailable and methylated, and how OM enhances or impedes Hg bioavailability.

Author contributions

D. Dabre: conceptualization, data curation, formal analysis, investigation, methodology, validation, writing – original draft, writing – review & editing. S. Guédron: conceptualization, data curation, formal analysis, methodology, resources, supervision, validation, writing – original draft, writing – review & editing. Y. Maiga: methodology, supervision, writing – review & editing. S. Jelavic: data curation, methodology, validation, review & editing. S. Campillo: data curation, formal analysis & methodology. J. Fin: data curation, formal analysis & methodology. S. Sentenac: data curation, formal analysis & methodology. O. Bruneel: methodology, supervision, writing – review & editing. O. Ouedraogo: methodology, supervision, writing – review & editing. R. Mason: data curation, formal analysis, methodology, supervision, writing – review & editing.

Conflicts of interest

There are no conflicts to declare.

Data availability

The data supporting this article have been included as part of the SI. See DOI: **https://doi.org/10.1039/d5em00426h**.

Acknowledgements

This research is the product of a joint project between the University Joseph KI-ZERBO (Ouagadougou, Burkina Faso) and the French National Research Institute for Sustainable Development (IRD, France). This publication was made possible through support provided by the African centers of excellence (ACE Partner – IRD and AFD) and by a grant from LabEx-OSUG@2020 (Investissements d'avenir – ANR10 LABX56). S. Guédron, S. Campillo, S. Jelavic, J. Fin, and S. Santenac (ISTerre/IRD/UGA) are part of Labex OSUG@2020 (Investissements d'avenir e ANR10 LABX56). We thank the ANEEMAS (Agence Nationale d'Encadrement des Exploitations Minières Artisanales et Semi – mécanisés) in Burkina Faso for having authorized and supported this research, as well as the IRD Representation in Burkina Faso for their collaboration and support in the project. We would like to thank Jacques Gardon of Hydrosciences Montpellier for his guidance and advice, and Bruno Lanson of the Institut des Sciences de la Terre for his help with the mineralogical analysis of our samples. Our sincere thanks go to Pr A. S. Ouattara, the recently deceased director of the host laboratory at the Université Joseph kI-ZERBO, who provided us with the space needed for sample preparation. We also thank Dr Benjamin Sawadogo from IRD Burkina Faso, Pr Koussoubé Youssouf, Dr Cheick Omar Tidiane Compaoré, and Palé Dagoro from University Joseph KI-ZERBO, who gave us support during sampling campaigns in recognized Jahadist danger zones.

References

1 L. J. Esdaile and J. M. Chalker, The Mercury Problem in Artisanal and Small-Scale Gold Mining, *Chem.–Eur. J.*, 2018, **24**(27), 6905–6916.
2 C. Tomicic, D. Vernez, T. Belem and M. Berode, Human mercury exposure associated with small-scale gold mining in Burkina Faso, *Int. Arch. Occup. Environ. Health*, 2011, **84**(5), 539–546.

3 P. Black, M. Richard, R. Rossin and K. Telmer, Assessing occupational mercury exposures and behaviours of artisanal and small-scale gold miners in Burkina Faso using passive mercury vapour badges, *Environ. Res.*, 2017, **152**, 462–469.
4 AMAP/UNEP, Technical background report for the global mercury assessment 2018, Arctic Monitoring and Assessment Programme, Oslo, Norway/UN Environment Programe, Geneva, Switzerland, 2019.
5 M. Grimaldi, S. Guédron and C. Grimaldi, Impact of gold mining on mercury contamination and soil degradation in Amazonian ecosystems of French Guiana, in *Land-use Change Impacts on Soil Processes: Tropical and Savannah Ecosystems*, ed. Brearley F. Q. and Thomas A. D., CABI, UK, 1st edn, 2015, pp. 95–107, DOI: **10.1079/9781780642109.0095**.
6 B. Niane, S. Guédron, F. Feder, S. Legros, P. M. Ngom and R. Moritz, Impact of recent artisanal small-scale gold mining in Senegal: Mercury and methylmercury contamination of terrestrial and aquatic ecosystems, *Sci. Total Environ.*, 2019, **669**, 185–193.
7 O. Gyamfi, P. B. Sørensen, G. Darko, E. Ansah, K. Vorkamp and J. L. Bak, Contamination, exposure and risk assessment of mercury in the soils of an artisanal gold mining community in Ghana, *Chemosphere*, 2021, **267**, 128910.
8 J. R. Gerson, C. T. Driscoll, H. Hsu-Kim and E. S. Bernhardt, Senegalese artisanal gold mining leads to elevated total mercury and methylmercury concentrations in soils, sediments, and rivers, *Elem. Sci. Anth.*, 2018, **6**, 11.
9 B. Niane, R. Moritz, S. Guédron, P. M. Ngom, H. R. Pfeifer, I. Mall, *et al.*, Effect of recent artisanal small-scale gold mining on the contamination of surface river sediment: Case of Gambia River, Kedougou region, southeastern Senegal, *J. Geochem. Explor.*, 2014, **144**, 517–527.
10 K. B. Kouadio, E. Resongles, K. E. Ahoussi, Z. Ouattara, I. Konaté, N. Fayol, *et al.*, Environmental contamination by metals, metalloids, and cyanides in the historic and active ASGM area of Kokumbo in Côte d'Ivoire, *Environ. Sci. Pollut. Res.*, 2025, **32**, 13699–13725.
11 A. Adjorlolo-Gasokpoh, A. A. Golow and J. Kambo-Dorsa, Mercury in the Surface Soil and Cassava, Manihot esculenta (Flesh, Leaves and Peel) Near Goldmines at Bogoso and Prestea, Ghana, *Bull. Environ. Contam. Toxicol.*, 2012, **89**(6), 1106–1110.
12 A. K. Donkor, J. C. Bonzongo, V. K. Nartey and D. K. Adotey, Mercury in different environmental compartments of the Pra River Basin, Ghana, *Sci. Total Environ.*, 2006, **368**(1), 164–176.
13 P. Van Straaten, Mercury contamination associated with small-scale gold mining in Tanzania and Zimbabwe, *Sci. Total Environ.*, 2000, **259**(1–3), 103–113.
14 M. Rajaee, R. Long, E. Renne and N. Basu, Mercury Exposure Assessment and Spatial Distribution in A Ghanaian Small-Scale Gold Mining Community, *Int. J. Environ. Res. Public Health*, 2015, **12**(9), 10755–10782.
15 N. K. Asare-Donkor and A. A. Adimado, Influence of mining related activities on levels of mercury in water, sediment and fish from the Ankobra and Tano River basins in South Western Ghana, *Environ. Syst. Res.*, 2016, **5**(1), 5.
16 R. P. Mason, Z. Baumann, G. Hansen, K. M. Yao, M. Coulibaly and S. Coulibaly, An assessment of the impact of artisanal and commercial gold mining on mercury and methylmercury levels in the environment and fish in Cote d'Ivoire, *Sci. Total Environ.*, 2019, **665**, 1158–1167.
17 O. Ouédraogo and M. Amyot, Mercury, arsenic and selenium concentrations in water and fish from sub-Saharan semi-arid freshwater reservoirs (Burkina Faso), *Sci. Total Environ.*, 2013, **444**, 243–254.
18 G. M. Gadd, Microbial formation and transformation of organometallic and organometalloid compounds, *FEMS Microbiol. Rev.*, 1993, **11**(4), 297–316.
19 R. P. Mason, J. R. Reinfelder and F. M. M. Morel, Bioaccumulation of mercury and methylmercury, *Water, Air, Soil Pollut.*, 1995, **80**(1–4), 915–921.
20 J. M. Parks, A. Johs, M. Podar, R. Bridou, R. A. Hurt, S. D. Smith, *et al.*, The Genetic Basis for Bacterial Mercury Methylation, *Science*, 2013, **339**(6125), 1332–1335.
21 L. Alanoca, S. Guédron, D. Amouroux, S. Audry, M. Monperrus, E. Tessier, *et al.*, Synergistic effects of mining and urban effluents on the level and distribution of methylmercury in a shallow aquatic ecosystem of the Bolivian Altiplano, *Environ. Sci.: Processes Impacts*, 2016, **18**(12), 1550–1560.
22 S. Guedron, S. Grangeon, B. Lanson and M. Grimaldi, Mercury speciation in a tropical soil association; Consequence of gold mining on Hg distribution in French Guiana, *Geoderma*, 2009, **153**(3–4), 331–346.
23 S. Guedron, M. Grimaldi, C. Grimaldi, D. Cossa, D. Tisserand and L. Charlet, Amazonian former gold mined soils as a source of methylmercury: Evidence from a small scale watershed in French Guiana, *Water Res.*, 2011, **45**(8), 2659–2669.
24 S. Guédron, S. Audry, D. Acha, S. Bouchet, D. Point, T. Condom, *et al.*, Diagenetic production, accumulation and sediment-water exchanges of methylmercury in contrasted sediment facies of Lake Titicaca (Bolivia), *Sci. Total Environ.*, 2020, **723**, 138088.
25 C. C. Gilmour, M. Podar, A. L. Bullock, A. M. Graham, S. D. Brown, A. C. Somenahally, *et al.*, Mercury Methylation by Novel Microorganisms from New Environments, *Environ. Sci. Technol.*, 2013, **47**(20), 11810–11820.
26 J. O. Nriagu, M. L. Blankson and K. Ocran, Childhood lead poisoning in Africa: a growing public health problem, *Sci. Total Environ.*, 1996, **181**(2), 93–100.
27 A. Bretzler, F. Lalanne, J. Nikiema, J. Podgorski, N. Pfenninger, M. Berg, *et al.*, Groundwater arsenic contamination in Burkina Faso, West Africa: Predicting and verifying regions at risk, *Sci. Total Environ.*, 2017, **584–585**, 958–970.
28 T. Fowe, H. Karambiri, J. E. Paturel, J. C. Poussin and P. Cecchi, Water balance of small reservoirs in the Volta

basin: A case study of Boura reservoir in Burkina Faso, *Agric. Water Manage.*, 2015, **152**, 99–109.
29 K. Kirk Woodman, L. Baratoux, A. Somda and L. Siebenaller, The Youga gold deposit, Burkina Faso, *Ore Geol. Rev.*, 2016, **78**, 631–638.
30 M. Robertson and L. Peters, West African Goldfields, *Episodes*, 2016, **39**(2), 155–176.
31 J. Némery, V. Mano, A. Coynel, H. Etcheber, F. Moatar, M. Meybeck, *et al.*, Carbon and suspended sediment transport in an impounded alpine river (Isère, France), *Hydrol. Processes*, 2013, **27**(17), 2498–2508.
32 N. Doebelin and R. Kleeberg, *Profex*: a graphical user interface for the Rietveld refinement program*BGMN*, *J. Appl. Crystallogr.*, 2015, **48**(5), 1573–1580.
33 W. C. Nugraha, H. Jeong, D. Q. Phan, Y. Ishibashi and K. Arizono, Combination of Vortex Agitation and Ultrasonic Irradiation for Mercury Removal from Sediment by Acid Extraction, *Bull. Environ. Contam. Toxicol.*, 2022, **108**(6), 1118–1123.
34 U.S. Environmental Protection Agency, Methyl Mercury in Water by Distillation, Aqueous Ethylation, Purge and Trap, and Cold Vapor Atomic Fluorescence Spectrometry (Method 1630), 1998.
35 K. M. Munson, D. Babi and C. H. Lamborg, Determination of monomethylmercury from seawater with ascorbic acid-assisted direct ethylation, *Limnol. Oceanogr.: Methods*, 2014, **12**(1), 1–9.
36 S. Guédron, D. Point, D. Acha, S. Bouchet, P. A. Baya, E. Tessier, *et al.*, Mercury contamination level and speciation inventory in Lakes Titicaca & Uru-Uru (Bolivia): Current status and future trends, *Environ. Pollut.*, 2017, **231**, 262–270.
37 S. Guédron, C. Duwig, B. L. Prado, D. Point, M. G. Flores and C. Siebe, (Methyl)Mercury, Arsenic, and Lead Contamination of the World's Largest Wastewater Irrigation System: the Mezquital Valley (Hidalgo State—Mexico), *Water, Air, Soil Pollut.*, 2014, **225**(8), 1–19.
38 C. R. Hammerschmidt and W. F. Fitzgerald, Geochemical Controls on the Production and Distribution of Methylmercury in Near-Shore Marine Sediments, *Environ. Sci. Technol.*, 2004, **38**(5), 1487–1495.
39 C. R. Hammerschmidt and W. F. Fitzgerald, Formation of Artifact Methylmercury during Extraction from a Sediment Reference Material, *Anal. Chem.*, 2001, **73**(24), 5930–5936.
40 M. Horvat, A modified method for the determination of methylmercury by gas chromatography, *Talanta*, 1990, **37**(2), 207–212.
41 L. Liang, N. S. Bloom and M. Horvat, Simultaneous determination of mercury speciation in biological materials by GC/CVAFS after ethylation and room-temperature precollection, *Clin. Chem.*, 1994, **40**(4), 602–607.
42 R. Falciani, E. Novaro, M. Marchesini and M. Gucciardi, Multi-element analysis of soil and sediment by ICP-MS after a microwave assisted digestion method, *J. Anal. At. Spectrom.*, 2000, **15**(5), 561–565.
43 S. Melaku, R. Dams and L. Moens, Determination of trace elements in agricultural soil samples by inductively coupled plasma-mass spectrometry: Microwave acid digestion versus aqua regia extraction, *Anal. Chim. Acta*, 2005, **543**(1–2), 117–123.
44 C. Rutz, L. Schmolke, V. Gvilava and C. Janiak, Anion Analysis of Ionic Liquids and Ionic Liquid Purity Assessment by Ion Chromatography, *Z. Anorg. Allg. Chem.*, 2017, **643**(1), 130–135.
45 D. Tisserand, D. Daval, L. Truche, A. Fernandez-Martinez, G. Sarret, L. Spadini, *et al.*, Recommendations and good practices for dissolved organic carbon (DOC) analyses at low concentrations, *MethodsX*, 2024, **12**, 102663.
46 D. Tisserand, S. Guédron, E. Viollier, D. Jézéquel, S. Rigaud, S. Campillo, *et al.*, Mercury, organic matter, iron, and sulfur co-cycling in a ferruginous meromictic lake, *Appl. Geochem.*, 2022, **146**, 105463.
47 S. Guédron, J. Tolu, E. Brisset, P. Sabatier, V. Perrot, S. Bouchet, *et al.*, Late Holocene volcanic and anthropogenic mercury deposition in the western Central Andes (Lake Chungará, Chile), *Sci. Total Environ.*, 2019, **662**, 903–914.
48 C. C. Windmöller, N. C. Silva, P. H. Morais Andrade, L. A. Mendes and C. Magalhães Do Valle, Use of a direct mercury analyzer® for mercury speciation in different matrices without sample preparation, *Anal. Methods*, 2017, **9**(14), 2159–2167.
49 H. Biester and C. Scholz, Determination of Mercury Binding Forms in Contaminated Soils: Mercury Pyrolysis versus Sequential Extractions, *Environ. Sci. Technol.*, 1997, **33**(1), 233–239.
50 F. Meloni, P. L. Higueras, J. Cabassi, B. Nisi, D. Rappuoli and O. Vaselli, Thermal desorption technique to speciate mercury in carbonate, silicate, and organic-rich soils, *Chemosphere*, 2024, **365**, 143349.
51 R. C. Rodríguez Martín-Doimeadios, J. C. Wasserman, L. F. García Bermejo, D. Amouroux, J. J. Berzas Nevado and O. F. X. Donard, Chemical availability of mercury in stream sediments from the Almadén area, Spain, *J. Environ. Monit.*, 2000, **2**(4), 360–366.
52 N. S. Bloom, E. Preus, J. Katon and M. Hiltner, Selective extractions to assess the biogeochemically relevant fractionation of inorganic mercury in sediments and soils, *Anal. Chim. Acta*, 2003, **479**(2), 233–248.
53 J. E. Kostka and G. W. Luther, Partitioning and speciation of solid phase iron in saltmarsh sediments, *Geochim. Cosmochim. Acta*, 1994, **58**(7), 1701–1710.
54 R. Raiswell, H. P. Vu, L. Brinza and L. G. Benning, The determination of labile Fe in ferrihydrite by ascorbic acid extraction: Methodology, dissolution kinetics and loss of solubility with age and de-watering, *Chem. Geol.*, 2010, **278**(1–2), 70–79.
55 M. M. Veiga, R. F. Baker, M. B. Fried and D. Withers, *Protocols for Environmental and Health Assessment of Mercury Released by Artisanal and Small-Scale Gold Miners*, Global Mercury Project, UNIDO, Vienna, 2004.

56 R. Webster, Statistics to support soil research and their presentation, *Eurasian J. Soil Sci.*, 2001, **52**(2), 331–340.
57 J. M. Bigham and D. K. Nordstrom, Iron and Aluminum Hydroxysulfates from Acid Sulfate Waters, *Rev. Mineral. Geochem.*, 2000, **40**(1), 351–403.
58 E. C. Dos Santos, J. C. De Mendonça Silva and H. A. Duarte, Pyrite Oxidation Mechanism by Oxygen in Aqueous Medium, *J. Phys. Chem. C*, 2016, **120**(5), 2760–2768.
59 O. Akoto, N. Bortey-Sam, Y. Ikenaka, S. M. M. Nakayama, E. Baidoo, Y. B. Yohannes, *et al.*, Contamination Levels and Sources of Heavy Metals and a Metalloid in Surface Soils in the Kumasi Metropolis, Ghana, *J. Health Pollut.*, 2017, **7**(15), 28–39.
60 A. J. Adewumi and T. A. Laniyan, Contamination, sources and risk assessments of metals in media from Anka artisanal gold mining area, Northwest Nigeria, *Sci. Total Environ.*, 2020, **718**, 137235.
61 G. M. A. Leiva and S. Morales, Environmental assessment of mercury pollution in urban tailings from gold mining, *Ecotoxicol. Environ. Saf.*, 2013, **90**, 167–173.
62 A. Sako and M. Nimi, Environmental geochemistry and ecological risk assessment of potentially harmful elements in tropical semi-arid soils around the Bagassi South artisanal gold mining site, *Cogent Environ. Sci.*, 2018, **4**(1), 1543565.
63 B. J. Alloway, *Heavy Metals in Soils*, Blackie academic & professional, London Glasgow Weinheim, 2nd edn, 1995.
64 V. P. Salonen and K. Korkka-Niemi, Influence of parent sediments on the concentration of heavy metals in urban and suburban soils in Turku, Finland, *Appl. Geochem.*, 2007, **22**(5), 906–918.
65 S. N. Dos Santos and L. R. F. Alleoni, Reference values for heavy metals in soils of the Brazilian agricultural frontier in Southwestern Amazônia, *Environ. Monit. Assess.*, 2013, **185**(7), 5737–5748.
66 M. R. Alfaro, A. Montero, O. M. Ugarte, C. W. A. Do Nascimento, A. M. De Aguiar Accioly, C. M. Biondi, *et al.*, Background concentrations and reference values for heavy metals in soils of Cuba, *Environ. Monit. Assess.*, 2015, **187**(1), 4198.
67 A. T. Reis, J. P. Coelho, S. M. Rodrigues, R. Rocha, C. M. Davidson, A. C. Duarte, *et al.*, Development and validation of a simple thermo-desorption technique for mercury speciation in soils and sediments, *Talanta*, 2012, **99**, 363–368.
68 M. Rumayor, M. Diaz-Somoano, M. A. Lopez-Anton and M. R. Martinez-Tarazona, Mercury compounds characterization by thermal desorption, *Talanta*, 2013, **114**, 318–322.
69 A. T. Reis, J. P. Coelho, I. Rucandio, C. M. Davidson, A. C. Duarte and E. Pereira, Thermo-desorption: A valid tool for mercury speciation in soils and sediments?, *Geoderma*, 2015, **237–238**, 98–104.
70 M. Rumayor, M. A. Lopez-Anton, M. Díaz-Somoano and M. R. Martínez-Tarazona, A new approach to mercury speciation in solids using a thermal desorption technique, *Fuel*, 2015, **160**, 525–530.
71 M. Rumayor, M. A. Lopez-Anton, M. Díaz-Somoano, M. M. Maroto-Valer, J. H. Richard, H. Biester, *et al.*, A comparison of devices using thermal desorption for mercury speciation in solids, *Talanta*, 2016, **150**, 272–277.
72 S. Guédron, D. Tisserand, S. Garambois, L. Spadini, F. Molton, B. Bounvilay, *et al.*, Baseline investigation of (methyl)mercury in waters, soils, sediments and key foodstuffs in the Lower Mekong Basin: The rapidly developing city of Vientiane (Lao PDR), *J. Geochem. Explor.*, 2014, **143**, 96–102.
73 S. Guédron, S. Devin and D. A. L. Vignati, Total and methylmercury partitioning between colloids and true solution: From case studies in sediment overlying and porewaters to a generalized model, *Environ. Toxicol. Chem.*, 2015, **35**(2), 330–339.
74 S. K. Verma and S. Chaurasia, Implicating the effects of consuming water with a high level of arsenic content: highlighting the cause and consequences of arsenic contamination in drinking water, *Water Pract. Technol.*, 2024, **19**(4), 1071–1083.
75 I. Somé, A. Sakira, M. Ouédraogo, T. Ouédraogo, A. Traoré, B. Sondo, *et al.*, Arsenic levels in tube-wells water, food, residents' urine and the prevalence of skin lesions in Yatenga province, Burkina Faso, *Interdiscip. Toxicol.*, 2012, **5**(1), 38–41.
76 J. F. Nzihou, M. Bouda, S. Hamidou and J. Diarra, Arsenic in Drinking Water Toxicological Risk Assessment in the North Region of Burkina Faso, *J. Water Resour. Prot.*, 2013, **05**(08), 46–52.
77 World Health Organization, Guidelines for drinking-water quality: fourth edition incorporating first addendum, 1st add, Geneva, World Health Organization, 4th edn, 2017, p. 541, **https://iris.who.int/handle/10665/254637**.
78 M. F. Naujokas, B. Anderson, H. Ahsan, H. V. Aposhian, J. H. Graziano, C. Thompson, *et al.*, The Broad Scope of Health Effects from Chronic Arsenic Exposure: Update on a Worldwide Public Health Problem, *Environ. Health Perspect.*, 2013, **121**(3), 295–302.
79 N. J. McNab, J. C. Hughes and J. R. Howard, Pollution effects of wastewater sludge application to sandy soils with particular reference to the behaviour of mercury, *Appl. Geochem.*, 1997, **12**(3), 321–325.
80 A. P. Martin, R. E. Turnbull, C. W. Rissmann and P. Rieger, Heavy metal and metalloid concentrations in soils under pasture of southern New Zealand, *Geoderma Reg.*, 2017, **11**, 18–27.
81 K. MacSween and G. C. Edwards, The role of precipitation and soil moisture in enhancing mercury air-surface exchange at a background site in south-eastern Australia, *Atmos. Environ.*, 2021, **255**, 118445.
82 A. Martínez-Cortizas, X. Pontevedra-Pombal, E. García-Rodeja, J. C. Nóvoa-Muñoz and W. Shotyk, Mercury in a Spanish Peat Bog: Archive of Climate Change and Atmospheric Metal Deposition, *Science*, 1999, **284**(5416), 939–942.
83 S. M. Gustin, M. Coolbaugh, M. Engle, B. Fitzgerald, R. Keislar, S. Lindberg, *et al.*, Atmospheric mercury

emissions from mine wastes and surrounding geologically enriched terrains, *Environ. Geol.*, 2003, **43**(3), 339–351.

84 P. Avotins, *Sciences SUD of AE. Adsorption and Coprecipitation Studies of Mercury on Hydrous Iron Oxide*, Stanford University, 1975, p. 248, Available from: **https://books.google.fr/books?id=4uc_AAAAIAAJ**.

85 C. Tiffreau, J. Lützenkirchen and P. Behra, Modeling the Adsorption of Mercury(II) on (Hydr)oxides, *J. Colloid Interface Sci.*, 1995, **172**(1), 82–93.

86 P. Trivedi and L. Axe, Ni and Zn Sorption to Amorphous versus Crystalline Iron Oxides: Macroscopic Studies, *J. Colloid Interface Sci.*, 2001, **244**(2), 221–229.

87 M. Fan, T. Boonfueng, Y. Xu, L. Axe and T. A. Tyson, Modeling Pb sorption to microporous amorphous oxides as discrete particles and coatings, *J. Colloid Interface Sci.*, 2005, **281**(1), 39–48.

88 I. Reyes and J. Torrent, Citrate-Ascorbate as a Highly Selective Extractant for Poorly Crystalline Iron Oxides, *Soil Sci. Soc. Am. J.*, 1997, **61**(6), 1647–1654.

89 T. Rennert, Wet-chemical extractions to characterise pedogenic Al and Fe species – a critical review, *Soil Res.*, 2019, **57**(1), 1.

90 M. Roulet, Methylmercury production and accumulation in sediments and soils of an Amazonian floodplain - effet of seasonal inundation, *Water, Air, Soil Pollut.*, 2001, **128**(1), 41–60.

91 A. H. Fostier, D. Amouroux, E. Tessier, J. L. M. Viana and L. Richter, Methylmercury content in soil and litter from the Amazonian rainforest and its potential fate during forest fires, *Front. Environ. Chem.*, 2023, **4**, 1242915.

92 J. R. Gerson, N. Szponar, A. A. Zambrano, B. Bergquist, E. Broadbent, C. T. Driscoll, *et al.*, Amazon forests capture high levels of atmospheric mercury pollution from artisanal gold mining, *Nat. Commun.*, 2022, **13**(1), 559.

93 J. R. Ikingura and H. Akagi, Total mercury and methylmercury levels in fish from hydroelectric reservoirs in Tanzania, *Sci. Total Environ.*, 2003, **304**(1–3), 355–368.

94 A. G. Bravo, S. Bouchet, S. Guédron, D. Amouroux, J. Dominik and J. Zopfi, High methylmercury production under ferruginous conditions in sediments impacted by sewage treatment plant discharges, *Water Res.*, 2015, **80**, 245–255.

95 B. Muresan, D. Cossa, S. Richard and Y. Dominique, Monomethylmercury sources in a tropical artificial reservoir, *Appl. Geochem.*, 2008, **23**(5), 1101–1126.

96 J. Hellal, S. Guédron, L. Huguet, J. Schäfer, V. Laperche, C. Joulian, *et al.*, Mercury mobilization and speciation linked to bacterial iron oxide and sulfate reduction: A column study to mimic reactive transfer in an anoxic aquifer, *J. Contam. Hydrol.*, 2015, **180**, 56–68.

97 T. A. Jackson, The influence of clay minerals, oxides, and humic matter on the methylation and demethylation of mercury by micro-organisms in freshwater sediments, *Appl. Organomet. Chem.*, 1989, **3**(1), 1–30.

98 S. M. Ullrich, T. W. Tanton and S. A. Abdrashitova, Mercury in the Aquatic Environment: A Review of Factors Affecting Methylation, *Crit. Rev. Environ. Sci. Technol.*, 2001, **31**(3), 241–293.

99 J. M. Benoit, C. C. Gilmour and R. P. Mason, The Influence of Sulfide on Solid-Phase Mercury Bioavailability for Methylation by Pure Cultures of *Desulfobulbus propionicus* (1pr3), *Environ. Sci. Technol.*, 2001, **35**(1), 127–132.

100 L. Lambertsson and M. Nilsson, Organic Material: The Primary Control on Mercury Methylation and Ambient Methyl Mercury Concentrations in Estuarine Sediments, *Environ. Sci. Technol.*, 2006, **40**(6), 1822–1829.

101 S. Bouchet, M. Goñi-Urriza, M. Monperrus, R. Guyoneaud, P. Fernandez, C. Heredia, *et al.*, Linking Microbial Activities and Low-Molecular-Weight Thiols to Hg Methylation in Biofilms and Periphyton from High-Altitude Tropical Lakes in the Bolivian Altiplano, *Environ. Sci. Technol.*, 2018, **52**(17), 9758–9767.

102 R. Q. Yu, J. R. Flanders, E. E. Mack, R. Turner, M. B. Mirza and T. Barkay, Contribution of Coexisting Sulfate and Iron Reducing Bacteria to Methylmercury Production in Freshwater River Sediments, *Environ. Sci. Technol.*, 2012, **46**(5), 2684–2691.

103 Y. Si, Y. Zou, X. Liu, X. Si and J. Mao, Mercury methylation coupled to iron reduction by dissimilatory iron-reducing bacteria, *Chemosphere*, 2015, **122**, 206–212.

